Accelerated Publication

THE JOURNAL OF BIOLOGICAL CHEMISTRY
Vol. 279, No. 36, Issue of September 3, pp. 37223–37226, 2004

Myosin VI Steps via a Hand-over-Hand Mechanism with Its Lever Arm Undergoing Fluctuations when Attached to Actin*

Received for publication, June 1, 2004,
and in revised form, June 24, 2004
Published, JBC Papers in Press, July 14, 2004,
DOI 10.1074/jbc.C400252200

Ahmet Yildiz‡§, Hyokeun Park‡§, Dan Safer¶, Zhaohui Yang¶, Li-Qiong Chen¶, Paul R. Selvin‡‖, and H. Lee Sweeney¶**

From the ‡Center for Biophysics and Computational Biology, Loomis Laboratory, University of Illinois, Urbana, Illinois 61801 and the ¶Department of Physiology, University of Pennsylvania School of Medicine, Philadelphia, Pennsylvania 19104-6085

Myosin VI is a reverse direction myosin motor that, as a dimer, moves processively on actin with an average center-of-mass movement of ~30 nm for each step. We labeled myosin VI with a single fluorophore on either its motor domain or on the distal of two calmodulins (CaMs) located on its putative lever arm. Using a technique called FIONA (fluorescence imaging with one nanometer accuracy), step size was observed with a standard deviation of <1.5 nm, with 0.5-s temporal resolution, and observation times of minutes. Irrespective of probe position, the average step size of a labeled head was ~60 nm, strongly supporting a hand-over-hand model of motility and ruling out models in which the unique myosin VI insert comes apart. However, the CaM probe displayed large spatial fluctuations (presence of ATP but not ADP or no nucleotide) around the mean position,whereas the motor domain probe did not. This supports a model of myosin VI motility in which the lever arm is either mechanically uncoupled from the motor domain or is undergoing reversible isomerization for part of its motile cycle on actin.

The myosin superfamily is composed of 18 classes of molecular motor proteins, the vast majority of which traffic toward the barbed (+) end of actin filaments (1). Class VI myosins were the first of the superfamily identified to traffic toward the pointed (−) end of the actin filament (2). They were first identified in *Drosophila melanogaster* (3) and are expressed from *Caenorhabditis elegans* to human (4–6). In addition to its unusual directionality, myosin VI has a number of additional unusual features. Single molecules of two-headed myosin VI, like myosin V, are capable of taking multiple steps (processive movement) on an actin filament without detachment (7). However, while myosin V has been demonstrated to move along actin filaments in 36-nm steps using its long lever arm (containing six calmodulins (CaMs)[1]) via a hand-over-hand mechanism (8–12), myosin VI does not appear to use a simple lever arm mechanism for its motility (7, 13). Myosin VI has been shown recently to have only two CaMs bound to each head (14), which should result in a short effective lever arm and small step size. Surprisingly, myosin VI has a step size that is highly variable (7) but on average nearly as large as that of myosin V, which has a lever arm that is three times longer. The variability of the step size has led to the postulate that myosin VI contains a long elastic element that allows it to undergo biased diffusion on an actin filament. The elastic element could be attached to the short lever arm, and/or the lever arm itself could become loosely attached to the motor at some point in the motile ATPase cycle. It was initially postulated that the unique insert of 39 amino acids in myosin VI that precedes the IQ motif (CaM-binding site) might come apart to form this flexible linker during the motile cycle on actin (7). This would result in the CaM being significantly displaced from the motor domain.

EM images of two-headed myosin V bound to actin show the two heads attached to actin monomers that are 36 nm apart, equivalent to the measured step size (15). In contrast, the only published EM images of two-headed myosin VI bound to actin appear to show the two heads bound to adjacent actin monomers (13). This raises the possibility that myosin VI might use an inchworm mechanism, or some related mechanism (13), in which one head is always the lead head. Thus the stepping mechanism of myosin VI is totally unclear.

Another surprising recent finding is that expressed full-length myosin VI molecules do not dimerize (16). This raises the possibility that dimerization is a regulated process for this motor *in vivo*, perhaps analogous to the kinesin family member, Unc104 (17). Single-headed, full-length myosin VI molecules were shown to have a non-processive movement (stroke) of ~18 nm (16). The authors of the study suggested that this could be due to a conventional lever arm of ~10 nm going through a 180° rotation. However, it is unclear how the properties of the monomeric motor are related to the behavior of the dimer.

To attempt to clarify the nature of the myosin VI stepping mechanism, we have applied the same technique that was developed and used to demonstrate a hand-over-hand mechanism for myosin V motility (8). This technique has been termed fluorescence imaging with one nanometer accuracy (FIONA) and can track the position of a single fluorophore with ~1.5 nm resolution. By placing a fluorophore on either the motor domain or the IQ-bound calmodulin of one head of a two-headed myosin VI construct, we were able to address whether myosin VI uses a hand-over-hand mechanism. We also assessed whether or not there is a dissociation of structural elements proximal to the IQ-CaM from the motor domain during any part of the actin-bound ATPase cycle.

* This work was supported by grants from the National Institutes of Health (to P. R. S. and H. L. S.). The costs of publication of this article were defrayed in part by the payment of page charges. This article must therefore be hereby marked "*advertisement*" in accordance with 18 U.S.C. Section 1734 solely to indicate this fact.

§ These authors contributed equally to this work.

‖ To whom correspondence may be addressed: Center for Biophysics and Computational Biology, Physics Dept. 1110, West Green St., Loomis Laboratory, University of Illinois, Urbana, IL 61801. E-mail: selvin@uiuc.edu.

** To whom correspondence may be addressed: Dept. of Physiology, University of Pennsylvania, A700 Richards Bldg., 3700 Hamilton Walk, Philadelphia, PA 19104-6085. Tel.: 215-898-8727; Fax: 215-573-2273; E-mail: lsweeney@mail.med.upenn.edu.

[1] The abbreviations used are: CaM, calmodulin; EM, electron micrograph; FIONA, fluorescence imaging with one nanometer accuracy; GFP, green fluorescent protein; eGFP, enhanced GFP.

MATERIALS AND METHODS

Protein Constructs and Expression—For the construction of the double-headed enhanced GFP (eGFP)-myosin VI construct, the eGFP cDNA (Clontech, Palo Alto, CA) was fused to the N terminus of the porcine myosin VI cDNA, which was truncated at Arg-994. This was followed by a leucine zipper (GCN4) to ensure dimerization and then a FLAG tag (encoding GDYKDDDDK) was included at the C terminus to facilitate purification (18). The construct was used to create a baculovirus for expression in Sf9 cells, as described previously (7, 19). To produce myosin VI dimers with only one eGFP-containing head, the virus coding for the eGFP heavy chain was co-infected with an unlabeled heavy chain at a ratio of 1:10. Assuming equal expression levels from the two viruses, this should result in a population that contains primarily unlabeled dimers, a small population of single eGFP-containing dimers, and virtually no double-labeled dimers.

For the Cy3-CaM-labeled constructs, chicken CaM with a single cysteine (Thr-146 → Cys) was expressed in *E. coli*. This expressed mutant CaM was labeled with Cy3. Unlabeled two-headed myosin VI was incubated with a mixture of unlabeled CaM and Cy3-CaM (ratio of 2:1). Exchange of the IQ-CaM was initiated by increasing the free [Ca^{2+}] to 100 μM. The concentration was then reduced to submicromolar, and unbound CaM was removed by gel filtration. The resulting myosin VI molecules had a single labeled CaM on one out of seven molecules.

Optics—All optics and data acquisition statistics used were previously described by Yildiz *et al.* (8). The only exception to this was the use of a 100 × 1.65 N.A. objective and associated sapphire coverslip (Olympus) used for the eGFP-myosin VI experiments. In addition, to ensure that polarization did not affect the results, the fluorophore emission was sent through a polarizing beam splitter (Dual View, Optical Insights Inc.), separating the orthogonal polarizations. The GFP-myosin VI and Cy3-myosin VI step sizes of each polarization were measured and found to be virtually identical to each other.

RESULTS AND DISCUSSION

Myosin-VI has a single "IQ motif" (calmodulin-binding site) following the motor domain and contains a coiled-coil region as well as a globular C-terminal tail (2, 5). Myosin VI also contains a unique insertion in between the motor domain and IQ motif, which recently was shown to be an unexpected binding site for a second calmodulin (14). As mentioned in the introduction, *in vitro* expression of full-length myosin VI does not result in a dimer, raising the possibility that the dimerization may be a regulated process *in vivo* (16).

When we initially constructed the dimer used in this study (2), we noted several peculiarities about the myosin VI coiled coil. First, based on Paircoil predictions, was the fact that the first 42 amino acids following the IQ motif (Leu-829 to Gln-871) had <50% of actually being coiled coil. This was followed by a 17 heptads of high probability coiled coil (Val-872 to Arg-994). However, nowhere in the coiled coil could we find a consensus trigger sequence (20), which would be necessary to initiate dimerization. Indeed, when a truncated myosin VI that ends at Arg-994 was expressed, dimers did not form (data not shown). Thus it is likely that dimerization is initiated by sequences distal to this coiled coil or perhaps even by other myosin VI-binding proteins.

Our previous experience with the smooth muscle rod (21) had demonstrated that the first 25 heptads of that coiled coil would not dimerize unless a trigger sequence was appended. In that study, as in this study, we appended GCN4, which contains a consensus trigger sequence (20) and will initiate dimerization of coiled coils lacking a trigger sequence. However, the myosin VI coiled coil is necessary for dimer stability, since when we remove all of the putative coiled coil from myosin VI and append only GCN4, dimers are not observed at the low concentrations (picomolar) of motor necessary for single molecule studies. This results in only single-headed encounters with actin in such assays (data not shown). To ensure that GCN4 did not alter the phasing of the coiled coil in a way that would influence the behavior of the motor domains of myosin VI, the GCN4 was inserted after the 12th heptad of coiled coil (ending at Arg-994). There are two predicted skips in the coiled coil between this heptad and the highest probability (~1) coiled coil (Gln-920 to Glu-954), which would prevent GCN4 from altering the phasing of the upstream coiled coil.

To place a fluorophore on the motor domain we created an eGFP-myosin VI fusion protein, with the eGFP at the N terminus of the motor. To selectively label only one of the two IQ-bound CaMs per double-headed molecule, we incubated labeled (Cy3) and unlabeled CaM (excess unlabeled) with myosin VI and then raised and lowered the free calcium concentration. Based on our previous work (14), we had observed that the first CaM is strongly bound to the unique insert with four Ca^{2+} at any Ca^{2+} concentration and is thus unaffected by changing Ca^{2+} concentration. (This was confirmed by the inability to exchange any labeled CaM onto an expressed myosin VI construct that lacked the IQ motif (data not shown).) On the other hand, four Ca^{2+} can bind and dissociate from the IQ-bound CaM. For this to occur, the IQ-CaM must transiently dissociate from its binding site and is thus free to exchange.

What we observed for both the eGFP and Cy3-CaM molecules clearly supports a hand-over-hand mechanism of movement. As shown in the raw traces and histograms of Fig. 1, *A* and *B*, the average step of the single labeled head was ~60 nm (see Fig. 1). While there was a skewing of the eGFP distribution to somewhat larger steps (63.3 ± 16.7 nm *versus* 55.2 ± 19.6 nm), this likely was an artifact due to the "blinking" of eGFP that caused many of the smaller steps to be unscored. (Note that the duration of the eGFP steps was shorter than for Cy3-CaM steps because the ATP concentration was higher. This was necessary to collect a sufficient number of steps before the eGFP photo-bleached.) For a hand-over-hand mechanism, this would imply that each of the two heads of the two-headed molecule is alternately taking ~30-nm steps. This agrees with the published optical trap data (7). An inchworm model would predict that the individual heads would take 30-nm steps, rather than the 60-nm steps that we observe. Also in agreement with the published myosin VI data is that the step size distribution is much broader than was seen for myosin V (8) (±19.6 nm for CaM-labeled myosin VI *versus* ± 5.3 nm for CaM-labeled myosin V), and back steps were observed. In addition, to confirm the hand-over-hand model, we plotted the dwell time histogram (8) of myosin VI. As expected, it shows the convolution of a ~60-nm step, intermingled with a 0-nm step (Fig. 2, *A* and *B*).

What was not observed (see *traces* in Fig. 1) was a large asymmetry in alternate steps. This would be expected if the unique insert that precedes the CaM comes apart to form a long, flexible tether during some part of the motile cycle on actin, as was proposed previously (7). The appearance of substeps within each large step (*i.e.* alternating 50- and 10-nm steps), correlated with the swing of the short myosin VI lever arm was also not observed (Fig. 1). Given the position of the Cy3-labeled CaM, the spatial resolution should be adequate to see a lever arm swing of greater than a few nanometers. It is possible that the linkage between the heads is compliant enough to allow most of the swing of the lead head to occur rapidly upon attachment to actin, and thus the movement is beyond the temporal resolution of our instrumentation (0.33–0.5 s). However, the compliance cannot be so great as to allow the entire swing, as this would prevent the kinetic "gating" than has been observed (19) (binding of ATP to the lead head is prevented until the rear head has detached).

A second possible explanation for lack of substeps is suggested by close examination of the data. Although the average step size did not differ between the molecules with eGFP on the

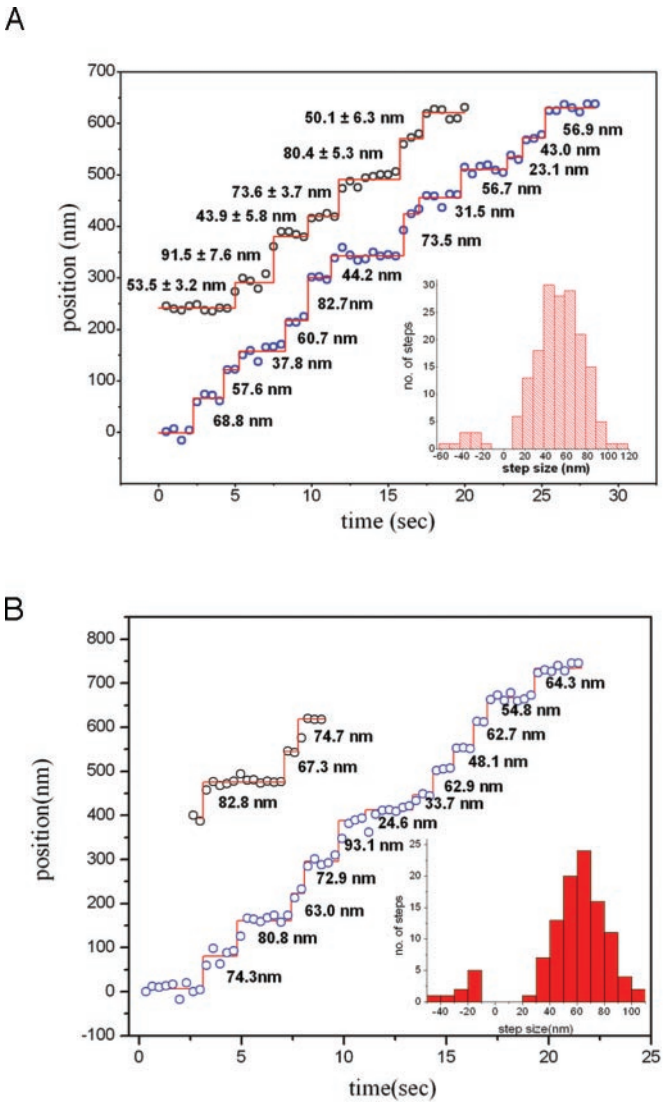

FIG. 1. **Step sizes of single fluorophore-labeled myosin VI.** *A*, stepping traces of two Cy3-labeled myosin VI molecules displaying average of ~60 nm steps. Histogram (*inset*) of a total of 33 myosin VIs taking 176 steps. The average forward step size measured is 55.2 ± 19.6 nm (n = 167), and backward step size is −31.7 ± 8.6 nm. *B*, stepping traces of an eGFP-labeled myosin VI molecules with step sizes. Histogram of step size (shown in the *right bottom inset*) shows forward and backward steps of myosin VI. The average of forward step sizes measured is 63.3 ± 16.7 nm, and the average of backward step sizes is 21.4 ± 11.2 nm. This histogram includes 107 steps of 31 myosin VI molecules.

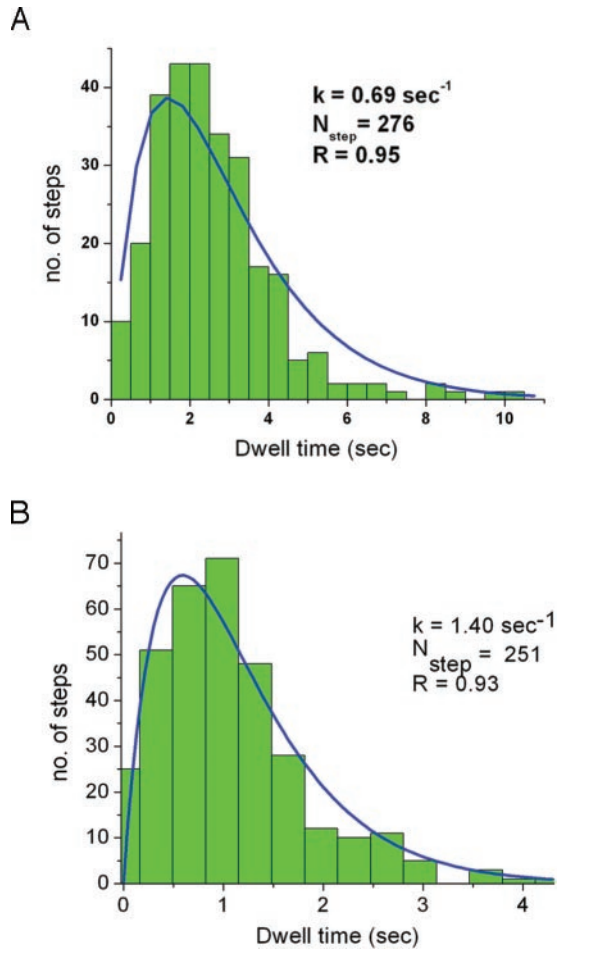

FIG. 2. **Dwell times of steps of single fluorophore-labeled myosin VI.** *A*, dwell time histogram of 36 myosin VIs taking 276 steps. Initial rise at short dwell period is indicative of myosin VI head takes 60-nm to 0-nm steps and the data fit well to the convolution function based on the kinetic hand-over-hand model, $P(t) = tk^2\, e^{-kt}$ (*blue line*) yielding coefficient of determination (R) = 0.95. Myosin VI takes 0.69 steps per second per molecule at 40 μM ATP. *B*, dwell time histogram of 52 myosin VIs taking 251 steps. The fit gives a rate constant k = 1.40 s^{-1} (r = 0.93) at 80 μM ATP, which is double of the rate constant of Cy3-CaM-labeled myosin VI at 40 μM ATP.

motor and Cy3 on the IQ-CaM, there was an important difference in the two sets of data. While the position of the eGFP-myosin VI motor showed very little spatial fluctuation, the Cy3-CaM oscillated around its mean position by ~7 nm. (Note that in the previous publication with labeled CaM on myosin V, such large spatial fluctuations were not seen, although asymmetric steps were seen (8).) This point was further explored by attaching the myosin VI-Cy3-CaM to actin either in the presence of MgADP (100 μM) or no nucleotide. In either case, the spatial fluctuations seen in the presence of MgATP were not present. In ADP or rigor, the standard deviation (σ) goes from 5 nm for an intensity of 200 photons to 3 nm for 600 photons. These numbers are in good agreement with the results that we reported for immobilized Cy3-DNA molecules on glass (8). However in ATP, σ is significantly larger (~7 nm) and stays relatively constant over the same intensity range, implying that in the ATP case, collecting more photons does not increase the resolution because the dye is highly mobile. If the ATP concentration was lowered to 0.1 μM, the fluctuations were essentially the same as in the absence of nucleotide.

This implies that the IQ-CaM of myosin VI is either uncoupled from the motor domain or is undergoing a reversible isomerization involving lever arm movement, during the myosin VI motile cycle on actin prior to ADP release. This likely involves a strongly actin-bound ADP state (or states) that is populated when going through the cycle but not populated by simple addition of ADP. The rearward strain (gating) provided by an attached rear head would greatly slow a lead head in such a state(s) from undergoing the structural transition necessary for product release. If the fluctuations are not due to a reversible isomerization, but to a physical uncoupling, then that uncoupling could occur either between the two CaMs, between the unique insert and the converter domain of the motor or perhaps between the converter domain and the rest of the motor. (Such an uncoupling of the converter has been seen in a crystal structure of scallop myosin II with MgADP bound (22).)

One can construct a model of the myosin VI stepping mechanism (Fig. 3) that incorporates these new findings and is consistent with the known kinetic scheme (19) of myosin VI. To have a net movement contributed by the lever arm of myosin

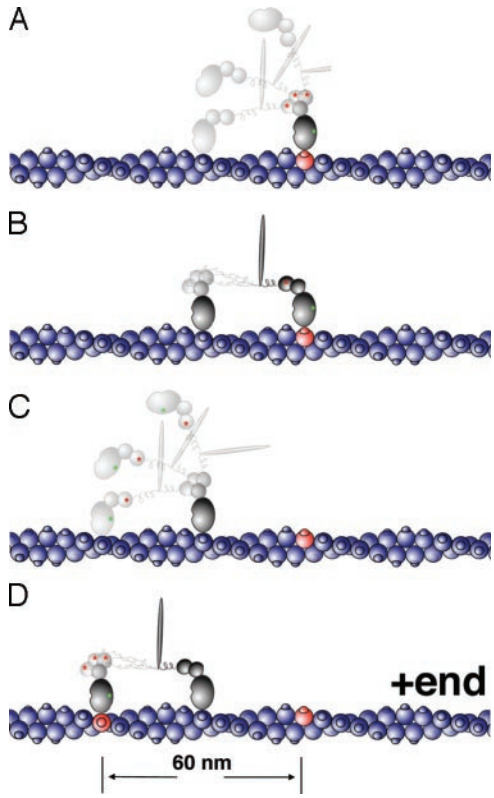

FIG. 3. **Model for the processive movement of two-headed myosin VI.** In all panels, the myosin VI motor domain is represented by the *large gray sphere* contacting the actin (*blue*) filament, while the two smaller spheres represent the two CaMs (lever arm) of each myosin VI head. The springs connecting the heads to the rod (representing the coiled coil) are the hypothetical missing extensible elements that the FIONA data suggest must follow the CaMs in the myosin VI structure. The *green asterisk* represents the motor domain position of the eGFP on one head, while the *red asterisk* represents the position of the Cy3 on one of the distal CaMs. *A*, hand-over-hand movement on actin is depicted, beginning with a labeled head bound and an unbound head (containing ADP·P_i) searching for a binding site. The bound, labeled head is undergoing fluctuations of its lever arm position. *B*, the unbound head binds to actin and rapidly releases P_i, while the rear head releases ADP. The lead head (ADP state) begins undergoing fluctuations in lever arm position, and ATP can bind and detach the labeled rear head. *C*, the detached (labeled) rear head hydrolyzes ATP and searches for next actin-binding site, on average 30 nm toward the pointed (−) end of the filament. *D*, the labeled head attaches as a lead head, releases P_I, and begins fluctuations. The head is again seen in the FIONA assay, but is now 60 nm from the previously visible location, as marked by the two *red* actin monomers.

VI, such a model must begin with a detached myosin VI head with ADP·P_i bound to the head and the lever arm pointing toward the barbed (+) end of the actin filament. When that head binds to actin, it rapidly releases the P_i and attaches with high affinity to actin. At this point the attached rear head prevents the lead head from reaching a sate that can rapidly release ADP, and the lever arm position of the lead head begins fluctuating. (Note, if the lead head was rapidly attaching and detaching in a weak actin-binding, ADP·P_i state, the motor position of a lead head would likely be seen on different actin monomers, rather than remaining bound to a single actin-binding site.) The lead head of an attached dimer is prevented from releasing ADP and/or binding ATP until the rear head detaches from actin (following ATP binding). This implies that the strain placed on a lead head by an attached rear head favors ADP remaining bound and disfavors ATP binding, which has been demonstrated in the optical trap (23). Once the rear head detaches, the mobility of the lever arm of the attached head would facilitate a diffusive search for an actin-binding site by the newly detached head. However, the fluctuations would allow the search to explore a larger number of potential actin sites than with a semi-rigid lever arm. The former lead head, now an unstrained rear head, can either strongly couple its lever arm to the motor, or reach an ADP state that allows release of ADP. Thus the rigor myosin VI rear head would have an immobilized lever arm, which is consistent with the cryo-EM reconstructions of single-headed myosin VI molecules (2).

The model described above partly can account for the variability in the myosin VI stepping, since the lever arm is undergoing fluctuations. However, it cannot fully account for the large size of the myosin VI steps. There must be structural elements that follow the IQ-CaM that extend the reach of the unbound head. Although this region has been assumed to be a part of a coiled coil, the first 42 amino acids following the IQ motif in fact have a very low probability of being coiled coil (Paircoil). This region could have some structure that effectively creates a longer lever arm, with most of the apparent flexibility of the myosin VI lever arm resulting from the uncoupling of the lever arm from the motor. Alternatively, this region could itself be a flexible tether to extend the distance of the diffusive search of an unbound head. Undoubtedly, there are more surprises to come with perhaps the most unconventional of the unconventional myosins, myosin VI.

Acknowledgments—We thank Anna Li and Damien Garbett for technical assistance in preparing the recombinant proteins.

REFERENCES

1. Berg, J. S., Powell, B. C., and Cheney, R. E. (2001) *Mol. Biol. Cell* **12,** 780–794
2. Wells, A. L., Lin, A. W., Chen, L.-Q., Safer, D., Cain, S. M., Hasson, T., Carragher, B. O., Milligan, R. A., and Sweeney, H. L. (1999) *Nature* **401,** 505–508
3. Kellerman, K. A., and Miller, K. G. (1992) *J. Cell Biol.* **119,** 823–834
4. Hasson, T., and Mooseker, M. S. (1994) *J. Cell Biol.* **127,** 425–440
5. Avraham, K. B., Hasson, T., Steel, K. P., Kingsley, D. M., Russell, L. B., Mooseker, M. S., Copeland, N. G., and Jenkins, N. A. (1995) *Nat. Genet.* **11,** 369–375
6. Avraham, K. B., Hasson, T., Sobe, T., Balsara, B., Testa, J. R., Skvorak, A. B., Morton, C. C., Copeland, N. G., and Jenkins, N. A. (1997) *Hum. Mol. Genet.* **6,** 1225–1231
7. Rock, R. S., Rice, S. E., Wells, A. L., Purcell, T. J., Spudich, J. A., and Sweeney, H. L. (2001) *Proc. Natl. Acad. Sci. U. S. A.* **98,** 13655–13659
8. Yildiz, A., Forkey, J. N., McKinney, S. A., Ha, T., Goldman, Y. E., and Selvin, P. R. (2003) *Science* **300,** 2061–2065
9. Mehta, A. D., Rock, R. S., Rief, M., Spudich, J. A., Mooseker, M. S., and Cheney, R. E. (1999) *Nature* **400,** 590–593
10. Forkey, J. N., Quinlan, M. E., Shaw, M. A., Corrie, J. E., and Goldman, Y. E. (2003) *Nature* **422,** 399–404
11. Purcell, T. J., Morris, C., Spudich, J. A., and Sweeney, H. L. (2002) *Proc. Natl. Acad. Sci. U. S. A.* **99,** 14159–14164
12. Sakamoto, T., Wang, F., Schmitz, S., Xu, Y., Molloy, J. E., Veigel, C., and Sellers, J. R. (2003) *J. Biol. Chem.* **278,** 29201–29207
13. Nishikawa, S., Homma, K., Komori, Y., Iwaki, M., Wazawa, T., Hikikoshi Iwane, A., Saito, J., Ikebe, R., Katayama, E., Yanagida, T., and Ikebe, M. (2002) *Biochem. Biophys. Res. Commun.* **290,** 311–317
14. Bahloul, A., Chevreux, G., Wells, A. L., Martin, D., Nolt, J., Yang, Z., Chen, L.-Q., Potier, N., Dorsselaer, A. V., Rosenfeld, S. S., Houdusse, A., and Sweeney, H. L. (2004) *Proc. Natl. Acad. Sci. U. S. A.* **101,** 4787–4792
15. Walker, M. L., Burgess, S. A., Sellers, J. R., Wang, F., Hammer, J. A., III, Trinick, J., and Knight, P. J. (2000) *Nature* **405,** 804–807
16. Lister, I., Schmitz, S., Walker, M., Trinick, J., Buss, F., Veigel, C., and Kendrick-Jones, J. (2004) *EMBO J.* **23,** 1729–1738
17. Al-Bassam, J., Cui, Y., Klopfenstein, D., Carragher, B. O., Vale, R. D., and Milligan, R. A. (2003) *J. Cell Biol.* **163,** 743–753
18. Hopp, T. P., Prickett, K. S., Price, V., Libby, R. T., March, C. J., Cerretti, P., Urdal, D. L., and Conlon, P. J. (1988) *Biotechnology* **6,** 1205–1210
19. De La Cruz, E. M., Ostap, E. M., and Sweeney, H. L. (2001) *J. Biol. Chem.* **276,** 32373–32381
20. Kammerer, R. A., Schulthess, T., Landwehr, R., Lustig, A., Engel, J., Aebi, U., Steinmetz, M. O. (1998) *Proc. Natl. Acad. Sci. U. S. A.* **95,** 13419–13424
21. Trybus, K. M., Freyzon, Y., Faust, L. Z., and Sweeney, H. L. (1997) *Proc. Natl. Acad. Sci. U. S.* A. **94,** 48–52
22. Houdusse, A., Kalabokis, V. N., Himmel, D., Szent-Gyorgyi, A. G., and Cohen, C. (1999) *Cell* **97,** 459–470
23. Altman, D., Sweeney, H. L., and Spudich, J. A. (2004) *Cell* **116,** 737–749